DEPTH-AVERAGED MODELING OF FLOW AND BED ELEVATION CHANGE IN A CURVED CHANNEL WITH DISPERSION STRESS TERMS

Dr. Tae Beom Kim [1], and Prof. Sung-Uk Choi [2]

[1] Researcher, Department of Civil and Environmental Engineering, Yonsei University, 134 Shinchon-dong, Seodaemun-gu, Seoul, Korea. Tel: ++ 82-2-2123-7889, geo108@naver.com
[2] Professor, Department of Civil and Environmental Engineering, Yonsei University, Seoul, Korea. schoi@yonsei.ac.kr

Abstract

The flow in curved channels is under the influence of centrifugal acceleration, which induces the secondary flow and the super-elevation in water surface. It is necessary to reflect these three dimensional flow characteristics on the 2D numerical model to simulate more accurately flows in curved channels. The purpose of this study is to develop a 2D finite element model which is capable of predicting the time-dependent flow and bed elevation change. The governing equations are the depth-averaged Reynolds equations for flow fields and the Exner's equation for bed deformation. In order to consider the secondary flow in curved channels, the effective stress terms are included in the momentum equations. The effective stress terms are composed of the turbulent stress and dispersion stress. The 2D CDG scheme is used for the numerical flow solution and classical BG scheme is used for the solution of Exner's equation. The developed model is a decoupled model in a sense that the bed elevation does not change simultaneously with the flow during each computational time step. For the accurate estimation of spatial variation of equilibrium sediment load, the effects of the secondary flows in a curved channel and the gravity force due to the geographic change on the direction of sediment transport are taken into account. For validation of flow model, flow experiment data and bed elevation change data in a 180° curved channel are used. At presently, this bed elevation change routine is restricted to the case with uniform sediment, neglecting armoring or grain sorting effects.
Key Words : Depth-averaged model, bed elevation change, curved channel, dispersion stress

1. INTRODUCTION

The flow in a curved channel is complicated and three dimensional due to secondary currents strengthened by the centrifugal force. So, in order to simulate numerically such flows correctly, a three-dimensional modeling, for example, Wu et al. [18], is required. However, two-dimensional models have been a favored choice by hydraulic engineers in practice because of their simplicity in implementation and application.

Molls and Chaudhry [14] proposed a numerical model based on the integrated effective stress, i.e., considering the turbulent viscosity as well as the fluid viscosity. Molls and Chaudhry applied the model to a bend flow experimented by Rozovskii [15] and obtained a moderate agreement. Lien et al. [13] simulated numerically bend flows by additionally considering the dispersion stress obtained from depth-averaging process. They showed that the dispersion stress plays a key role in the transverse momentum transfer from the inner to outer bank in a channel bend. Later, Hsieh and Yang [8] conducted numerical experiments using the model developed by Lien et al. [13] and demonstrated that the impact of secondary currents is serious in a bend flow. Lien et al. presented a guideline to describing the condition under which their bend flow model is necessary.

Recently, 2D FDM models using curvilinear coordinate system or 2D FVM are developed (Kassem and Chaudhry [10], Duc et al. [3], and Wu [18]) since Cartesian coordinate systems may not accurately represent the irregular channel shape and can induce inaccurate simulation results. It is well

known that the finite element method provides more flexibility in handling spatial domain than FDM or FVM. However, studies on the morphological change using the finite element model are rare.

In this study, a numerical model which is capable of predicting the time variation of the flow characteristics and bed elevation is proposed. The depth-averaged flow equations including the dispersion stress terms in momentum equation and the Exner's equation are solved by the finite element method. The shallow water equations are solved with 2D Characteristic Dissipative-Galerkin scheme proposed by Ghanem [5] which belongs to the family of the Streamline-Upwind / Petrov-Galerkin (SU/PG) scheme. The Exner's equation is solved with classical Bubnov-Galerkin scheme. The developed model is applied to 180° bended laboratory channel data for the validation of the proposed numerical model.

2. GOVERNING EQUATIONS

2.1 Flow Equations

For incompressible fluids, integrating the Reynolds equations leads to the following equations:

$$\frac{\partial h}{\partial t}+\frac{\partial p}{\partial x}+\frac{\partial q}{\partial y}=0 \tag{1}$$

$$\frac{\partial p}{\partial t}+\frac{\partial}{\partial x}\left(\frac{p^2}{h}+\frac{gh^2}{2}\right)+\frac{\partial}{\partial y}\left(\frac{pq}{h}\right)+gh\frac{\partial z_b}{\partial x}+\frac{1}{\rho}\tau_{bx}-\frac{\partial}{\partial x}\left(2\nu_t\frac{\partial p}{\partial x}\right)$$
$$-\frac{\partial}{\partial y}\left[\nu_t\left(\frac{\partial p}{\partial y}+\frac{\partial q}{\partial x}\right)\right]+\frac{\partial}{\partial x}\left[\int_{z_b}^{H}\left(\bar{u}-u\right)^2 dz\right]+\frac{\partial}{\partial y}\left[\int_{z_b}^{H}\left(\bar{u}-u\right)\left(\bar{v}-v\right)dz\right]=0 \tag{2}$$

$$\frac{\partial q}{\partial t}+\frac{\partial}{\partial x}\left(\frac{pq}{h}\right)+\frac{\partial}{\partial y}\left(\frac{q^2}{h}+\frac{gh^2}{2}\right)+gh\frac{\partial z_b}{\partial y}+\frac{1}{\rho}\tau_{by}-\frac{\partial}{\partial x}\left[\nu_t\left(\frac{\partial p}{\partial y}+\frac{\partial q}{\partial x}\right)\right]$$
$$-\frac{\partial}{\partial y}\left(2\nu_t\frac{\partial q}{\partial y}\right)+\frac{\partial}{\partial x}\left[\int_{z_b}^{H}\left(\bar{u}-u\right)\left(\bar{v}-v\right)dz\right]+\frac{\partial}{\partial y}\left[\int_{z_b}^{H}\left(\bar{v}-v\right)^2 dz\right]=0 \tag{3}$$

In the integration, the kinematic free surface and rigid impermeable boundary conditions are imposed, and the hydrostatic pressure distribution is assumed. In Eqs.(1)-(3), h is the water depth, $p\ (=uh)$ and $q\ (=vh)$ are flow discharge components per unit width in the x- and y-directions, respectively (here, u and v are depth-averaged velocity components in the x- and y-directions, respectively), g is the gravitational acceleration, z_b is the bottom elevation, H is the water surface elevation, ρ is the fluid density, τ_b is the bed shear stress, ν_t is the turbulent viscosity, and $\bar{u}$ and $\bar{v}$ are time-averaged velocity components in the x- and y-directions, respectively. The x- and y-components of the bed shear stress are, respectively, given by

$$\tau_{bx}=\frac{\rho g n^2}{h^{7/3}}p\left(p^2+q^2\right)^{1/2} \tag{4}$$

$$\tau_{by}=\frac{\rho g n^2}{h^{7/3}}q\left(p^2+q^2\right)^{1/2} \tag{5}$$

where n is the Manning's roughness coefficient. For turbulent viscosity, the following relationship is used.

$$\nu_t=\frac{\kappa}{6}U_* h \tag{6}$$

where κ is von Kármán constant (≈ 0.41) and U_* is the shear velocity.

The dispersion stress terms resulted from the integration of the product of the difference between the mean velocity and the true velocity distribution in a curved channel. The secondary flow in a curved channel is caused by the local imbalance between the centrifugal forces and the transverse pressure forces generated by superelevation of the water surface. The vertical distributions of the velocity are no longer uniform (Lien et al. [13]). De Vriend [1] proposed the relationship between the time-averaged and the depth-averaged velocity components by using perturbation method as following:

$$\bar{u} = u f_m(Z) - \delta h U f_s(Z) \tag{7}$$

$$\bar{v} = v f_m(Z) - \delta h V f_s(Z) \tag{8}$$

$$Z = \frac{z - H}{H - z_b}; [-1,\ 0] \tag{9}$$

$$f_m(Z) = 1 + \frac{\sqrt{g}}{\kappa C} + \frac{\sqrt{g}}{\kappa C}\ln(1+Z) \tag{10}$$

$$f_s(Z) = 2F_1(Z) + \frac{\sqrt{g}}{\kappa C}F_2(Z) - 2\left(1 - \frac{\sqrt{g}}{\kappa C}\right) f_m(Z) \tag{11}$$

$$F_1(Z) = \int_{-1+Z'}^{Z} \frac{\ln(1+Z)}{Z} dZ \tag{12}$$

$$F_2(Z) = \int_{-1+Z'}^{Z} \frac{\ln^2(1+Z)}{Z} dZ \tag{13}$$

$$Z' = \exp\left(-1 - \frac{\kappa C}{\sqrt{g}}\right) \tag{14}$$

$$U = \frac{1}{2\kappa^2 U^3}\left[\left(U^2 + v^2\right)\left(u\frac{\partial u}{\partial x} + v\frac{\partial u}{\partial y}\right) - uv\left(u\frac{\partial v}{\partial x} + v\frac{\partial v}{\partial y}\right)\right] \tag{15}$$

$$V = \frac{1}{2\kappa^2 U^3}\left[\left(U^2 + u^2\right)\left(u\frac{\partial v}{\partial x} + v\frac{\partial v}{\partial y}\right) - uv\left(u\frac{\partial u}{\partial x} + v\frac{\partial u}{\partial y}\right)\right] \tag{16}$$

$$U = \sqrt{u^2 + v^2} \tag{17}$$

$$\delta = \frac{\bar{h}}{\bar{R}} \tag{18}$$

where C is the Chézy's roughness coefficient, $\bar{h}$ is a characteristic depth of flow such as the overall average, and $\bar{R}$ is a characteristic radius of curvature such as the radius of curvature of the inner bank at some representative cross-section. Last two terms in Eq. (2) and (3) are the dispersion stress due to depth-averaging. By applying de Vriend's relationship from Eq. (7) to Eq. (18) to the dispersion stress terms in Eqs. (2) and (3), the integration within the dispersion stress terms can be rewritten as following:

$$\int_{z_b}^{H}\left(\bar{u} - u\right)^2 dz = u^2 h\left(\frac{\sqrt{g}}{\kappa C}\right)^2 - 2uUh^2\delta\frac{\sqrt{g}}{\kappa C}FF_1 + h^3\left(\delta U\right)^2 FF_2 \tag{19}$$

$$\int_{z_b}^{H}\left(\bar{u} - u\right)\left(\bar{v} - v\right)dz = uvh\left(\frac{\sqrt{g}}{\kappa C}\right)^2 - \left(uV + vU\right)h^2\delta\frac{\sqrt{g}}{\kappa C}FF_1 + h^3\delta^2 UVFF_2 \tag{20}$$

$$\int_{z_b}^{H}\left(\bar{v} - v\right)^2 dz = v^2 h\left(\frac{\sqrt{g}}{\kappa C}\right)^2 - 2vVh^2\delta\frac{\sqrt{g}}{\kappa C}FF_1 + h^3\left(\delta V\right)^2 FF_2 \tag{21}$$

$$FF_1 = \int_0^1 \left[\left(1 + \ln \xi\right) f_s\left(\xi\right) \right] d\xi \tag{22}$$

$$FF_2 = \int_0^1 \left[f_s\left(\xi\right) \right]^2 d\xi \tag{23}$$

$$f_s\left(\xi\right) = 2\int_0^\xi \frac{\ln t}{t-1} dt + \frac{\sqrt{g}}{\kappa C} \int_0^\xi \frac{\ln^2 t}{t-1} dt - 2\left(1 - \frac{\sqrt{g}}{\kappa C}\right)\left(1 + \frac{\sqrt{g}}{\kappa C} + \frac{\sqrt{g}}{\kappa C} \ln \xi\right) \tag{24}$$

Eqs. (22), (23), and (24) can be calculated by numerical integration method such as the Gauss quadrature formula. By applying Eqs. (19), (20), and (21) to Eqs. (2) and (3), the dispersion stress terms can be induced.

2.2 Exner's Equation

In order to estimate the bed elevation change, the following Exner's equation is solved:

$$\left(1 - p'\right) \frac{\partial z_b}{\partial t} + \frac{\partial q_{tx}}{\partial x} + \frac{\partial q_{ty}}{\partial y} = 0 \tag{25}$$

where p' is porosity, and q_{tx} and q_{ty} are the x- and y-components of total sediment load per unit width which are expressed as following, respectively.

$$q_{tx} = q_t \cos\Phi \,;\; q_{ty} = q_t \cos\Phi \tag{26}$$

where Φ is the counterclockwise angle of sediment transport direction from the positive x-axis , and q_t is total sediment load per unit width. In the present study, Engelund and Hansen's [4] formula is used for the total sediment load as following:

$$q_t = 0.05 \gamma_s V^2 \left[\frac{d}{g\left(\gamma_s / \gamma - 1\right)} \right]^{1/2} \left[\frac{\tau_0}{\left(\gamma_s - \gamma\right) d_{50}} \right]^{3/2} \tag{27}$$

where V is depth-averaged flow velocity, γ is specific weight of fluid, γ_s is specific weight of sediment, d_{50} is the median grain diameter, and τ_0 is bed shear stress.

In laterally sloping bed, sediment transport direction in Eq. (26) is not identical with the direction of bed shear stress due to the gravity force acting on the particles. This effect can be expressed as following (Koch and Flokstra [12]):

$$\tan\Phi = \frac{\sin\alpha - \dfrac{1}{f_s \theta_*} \dfrac{\partial z_b}{\partial y}}{\cos\alpha - \dfrac{1}{f_s \theta_*} \dfrac{\partial z_b}{\partial x}} \tag{28}$$

where α is the direction of bed shear stress, f_s is shape factor ranging from 1 to 2, and θ_* is the dimensionless Shield's parameter expressed as following:

$$\theta_* = \frac{n^2 V^2}{h^{1/3} \left(\dfrac{\gamma_s}{\gamma} - 1 \right) d_{50}} \tag{29}$$

In a curved channel, the difference of centrifugal forces between the upper and the lower layer of flow induces the secondary flow, also known as helical or spiral flow. The secondary flow causes the

direction of bed shear stress to deviate from the direction of the mean flow velocity. Therefore, it is necessary to reflect the effect of secondary flow on the sediment transport direction in a curved channel. This effect can be introduced in Eq. (28) as following:

$$\alpha = \tan^{-1}\left(\frac{v}{u}\right) + \tan^{-1}\left(\frac{Fh}{R_c}\right) \tag{30}$$

where R_c is the local radius of curvature of the streamline, and F is the parameter defined as following (Jansen [9]):

$$F = \frac{2}{\kappa^2}\left(1 - \frac{n\sqrt{g}}{\kappa h^{1/6}}\right) \tag{31}$$

In Eq. (30), the second term of the right side is the deviation of the bed shear stress from the streamlines due to the secondary flow in a curved channel. Since in some cases the inertia of the secondary flow has to be accounted for, it is necessary to reflect the inertia effects using an inertial adaptation equation (Struiksma et al. [16]) as following:

$$\beta \frac{C}{\sqrt{g}} h \frac{\partial I}{\partial s} + I = \frac{hV}{R} \tag{32}$$

$$I = \frac{hV}{R_c} \tag{33}$$

where I is a measure of the intensity of the secondary flow, s is the streamwise coordinate, β is a given coefficient normally between 0.4 and 2.0, for which de Vriend [2] proposed about 1.3 and Struiksma et al. [16] used 0.6, and R is the local radius of curvature of the streamline calculated as following:

$$\frac{1}{R} = \frac{1}{V^3}\left[\left(u^2 \frac{\partial v}{\partial x} + uv \frac{\partial v}{\partial y}\right) - \left(uv \frac{\partial u}{\partial x} + v^2 \frac{\partial u}{\partial y}\right)\right] \tag{34}$$

3. NUMERICAL METHODS

3.1 Flow Equations

To solve the flow equations numerically, the Streamline-Upwind/Petrov-Galerkin (SU/PG) scheme is used. The SU/PG scheme employs the weighting function as following:

$$N_i^* = N_i + \omega \Delta x \frac{\partial N_i}{\partial x} \mathbf{W_x} + \omega \Delta y \frac{\partial N_i}{\partial y} \mathbf{W_y} \tag{35}$$

where N_i is basis or shape function for the i-th node, N_i^* is weighting function for the i-th node, ω is weighting coefficient, and $\mathbf{W_x}$ and $\mathbf{W_y}$ are weighting matrices in the x- and y-directions, respectively. In this study, following weighting matrices suggested by Ghanem [5] are used:

$$\mathbf{W_x} = \frac{\mathbf{A}}{\sqrt{\mathbf{A}^2 + \mathbf{B}^2}}, \quad \mathbf{W_y} = \frac{\mathbf{B}}{\sqrt{\mathbf{A}^2 + \mathbf{B}^2}} \tag{36}$$

The inverse of the square root of the matrix can be determined by Cayley-Hamilton theorem (Hoger and Carlson [6]). In estimation of Δx and Δy, following expressions suggested by Katopodes [11], which can be applied to the distorted elements, are used:

$$\Delta x = 2\sqrt{\left(\frac{\partial x}{\partial \xi}\right)^2 + \left(\frac{\partial x}{\partial \eta}\right)^2}\ ,\ \Delta y = 2\sqrt{\left(\frac{\partial y}{\partial \xi}\right)^2 + \left(\frac{\partial y}{\partial \eta}\right)^2} \tag{37}$$

where ξ and η are isoparametric coordinates. Then, the weighted residual equation of the shallow water equations takes the form of

$$\begin{aligned}&\int_\Omega \left(N_i + \omega \Delta x \frac{\partial N_i}{\partial x}\mathbf{W_x} + \omega \Delta y \frac{\partial N_i}{\partial y}\mathbf{W_y} \right) \\ &\times \left(\frac{\partial \mathbf{U}}{\partial t} + \mathbf{A}\frac{\partial \mathbf{U}}{\partial x} + \mathbf{B}\frac{\partial \mathbf{U}}{\partial y} + \frac{\partial \mathbf{D_x}}{\partial x} + \frac{\partial \mathbf{D_y}}{\partial y} + \mathbf{F} \right) d\Omega = 0\end{aligned} \tag{38}$$

The resulting nonlinear equations are linearized by using the Newton-Raphson method, and the global matrix is solved by the frontal solution algorithm for unsymmetric matrices proposed by Hood [7].

3.2 Exner's Equation

The weighted residual equation of the Exner's equations for bed elevation change is as following:

$$\int_\Omega N^* \left[\frac{\partial z_b}{\partial t} + \frac{1}{1-p'}\left(\frac{\partial q_{tx}}{\partial x} + \frac{\partial q_{ty}}{\partial y} \right) \right] d\Omega = 0 \tag{39}$$

The time derivative is replaced by finite difference form and the finite element approximation to the solution or variables is applied. Then, the following equation in matrix form can be obtained by applying the Green's theorem in Eq. (39) and the finite element approximation to the solution:

$$\mathbf{A}\Delta\mathbf{z_b} = \frac{\Delta t}{1-p'}(\mathbf{D} - \mathbf{F}) \tag{40}$$

$$A_{ij} = \int_{\Omega^e} \left(N_i^* N_j \right) d\Omega^e \tag{41}$$

$$D_{ij} = \int_{\Omega^e} \left(\frac{\partial N_i^*}{\partial x} q_{tx} + \frac{\partial N_i^*}{\partial y} q_{ty} \right) d\Omega^e \tag{42}$$

$$F_i = \int_{\Gamma^e} \left[N_i^* \left(n_x q_{tx} + n_y q_{ty} \right) \right] d\Gamma^e \tag{43}$$

where Γ^e means the boundary of an element. In Eq. (39), time derivative can be replaced by time-difference approximation of the general form, as following:

$$\frac{z_b^{n+1} - z_b^n}{\Delta t} = \theta \left(\frac{\partial z_b}{\partial t} \right)^{n+1} + (1-\theta) \left(\frac{\partial z_b}{\partial t} \right)^n \tag{44}$$

where n is the know time level, n+1 is the unknown time level, and θ is the implicitness parameter.

4. VERIFICATIONS

4.1 Flow Characteristics in a 180° Curved Channel

For the validation of the flow routine, the developed model was applied to Rozovskii's [15] experiment. The channel bend consists of 180° curved reach with a 6 m long straight approach and 3 m long straight exit. The mean radius of the channel bend is 0.8 m with the internal and external radius of curvature of 0.4 m and 1.2 m, respectively. The cross section of the channel bend is a 0.8 m wide rectangle, and the entire channel bend is horizontal. The channel bottom is made smooth, and the

estimated Chézy's coefficient is 60 $m^{1/2}/s$. The discharge is 0.0123 m^3/s with a mean velocity of 0.265 m/s and a flow depth of 0.6 m. The Reynolds number and Froude number of the generated flow are 15,600 and 0.114, indicating a turbulent and subcritical flow. The set of data used in the present study is Experiment No.1 in the series of Rozovskii's bend flow experiments.

Figure 1 shows measured and simulated contour plots of water surface of Rozovskii's channel bend experiment. Figure 1(b) is the result of no dispersion stress and Figure 1(c) is the result with dispersion stress. It can be seen that the numerical model reproduces well the super-elevation in the channel bend, i.e., higher water surface elevation along the outer bank than along the inner bank. Overall agreement between measured and simulated profiles appears to be good. However, the simulated results are observed to be more symmetric in the bend than the measured data. Specifically, the numerical model cannot exactly simulate the maximum water surface decrease at the inner bank in the vicinity of 6.9 m cross section and maximum water surface increase at the outer bank around 7.4 m cross section from the upstream end. When the comparison point is focused on only 6.2 cm contour line, the result with dispersion stress in Figure 1(c) is better than that without dispersion stress in Figure 1(b). Figure 2 presents the longitudinal distributions of measured and simulated velocity. It can be seen that the numerical model simulates the flow acceleration along the inner bank very well. However, the computed velocity distribution is different from measured one at Section 8. Additionally, the simulated results cannot present the tendency that the velocity along the outer bank definitely becomes faster than that along the inner bank after the flow turns around the end of the bend. However, this tendency can faintly be seen in Figure 2(c).

4.2 Bed Elevation Change in a 180° Curved Channel

For validation of the bed elevation change routine, the developed model is applied to 180° curved channel data from Laboratory of Fluid Mechanics (LFM) in Delft University of Technology (Sutmuller and Glerum [17]). The channel bend consists of 180° curved reach with a 13.35 m. The mean radius of the channel bend is 4.25 m. The cross section of the channel bend is a 1.7 m wide rectangle, and the channel slope is 0.0018. The estimated Chézy's coefficient is 26.4 $m^{1/2}/s$. The discharge is 0.17 m^3/s with a mean velocity of 0.5 m/s and a flow depth of 0.2 m. The medium grain size of channel bottom is 0.78 mm.

Figure 3 shows the result of the bed elevation change normalized by the flow depth h_0 = 0.2 m after the equilibrium state. The simulated profile shows deposition and erosion near the inner and outer banks, respectively, which conforms to the measurement. However, the numerical model cannot predict exactly the location of the maximum deposition and erosion around section 10 in Figure 3(a). Figure 4 shows the super-elevation after the equilibrium state, which shows different tendency from the Figure 1. The contour line in Figure 1 is radial, but in Figure 4 is crossing the channel bend. This is due to the different channel geometry, such as channel width, radius of curvature, slope and so on, and the different flow characteristics.

5. CONCLUSIONS

In this study, 2D finite element numerical model in which the dispersion stress terms are added to the momentum equations in order to consider the secondary flow effects in a curved channel was developed. The dispersion stress could be induced by using the relationship between the time-averaged and depth-averaged velocity proposed by de Vriend [1]. The 2D CDG scheme which is a kind of SU/PG method was used for the numerical flow solution and classical BG scheme was used for the solution of Exner's equation. For the validation of developed model, Rozovskii's experiment data and LFM data were used for flow and bed elevation change, respectively. Overall agreement between measured and simulated results appeared to be good. However, closely compared, 2D numerical model could not exactly simulate the experimental results such as the maximum increase and decrease points of water surface and the maximum depositional and erosional location. Nevertheless, in view of the simulated results compared to the measurements, the one including the dispersion stress could simulate the flow characteristics more closely to the measurement than the other excluding the dispersion stress.

ACKNOWLEDGEMENTS

This research was supported by a grant (code No. 2-3-3) from Sustainable Water Resources Research Center of 21st Century Frontier Research Program.

REFERENCES

[1] De Vriend, H.J., (1977) : A mathematical model of steady flow in curved shallow channel, Journal of Hydraulic Research, 15(1), pp.37-54.

[2] De Vriend, H.J., (1981) : Steady flow in shallow channel bends, Communications on Hydraulics, Department Civil Engineering, Delft University of Technology, The Netherlands.

[3] Duc, B.M., Wenka, T. and Rodi, W., (2004) : Numerical modeling of bed deformation in laboratory channels, Journal of Hydraulic Engineering, ASCE, 130(9), pp.894-904.

[4] Engelund, F. and Hansen, E., (1972) : A monograph on sediment transport in alluvial streams, Copenhagen, Teknisk Forlag.

[5] Ghanem, A.H.M., (1995) : Two-dimensional finite element modeling of flow in aquatic habitats, Ph.D. dissertation, University of Alberta, Edmonton, Alberta.

[6] Hoger, A. and Carlson, D.E., (1984) : Determination of the stretch and rotation in the polar decomposition of the deformation gradient, Quarterly of Applied Mathematics, 42(1), pp.113-117.

[7] Hood, P., (1976) : Frontal solution program for unsymmetric matrices, International Journal of Numerical Methods in Engineering, 10, pp. 379-399.

[8] Hsieh, T.Y. and Yang, J.C., (2003) : Investigation on the suitability of two-dimensional depth-averaged models for bend-flow simulation, Journal of Hydraulic Engineering, ASCE, 129(8), pp.597-612.

[9] Jansen, P.P., (1979) : Principles of River Engineering, Pitman, London, pp.509.

[10] Kassem, A.A. and Chaudhry, M.H., (2002) : Numerical modeling of bed evolution in channel bend, Journal of Hydraulic Engineering, ASCE, 128(5), pp.507-514.

[11] Katopodes, N.D., (1984) : Two-dimensional surges and shocks in open channels, Journal of Hydraulic Engineering, ASCE, 110(6), pp.794-812.

[12] Koch, F.G. and Flokstra, C., (1981) : Bed level computations for curved alluvial channels, Proceedings of the XIXth Congress of the IAHR, New Delhi, India, pp.357-364.

[13] Lien, H.C., Hsieh, T.Y., Yang, J.C., and Yeh, K.C., (1999) : Bend-flow simulation using 2D depth-averaged model, Journal of Hydraulic Engineering, ASCE, 125(10), pp.1097-1108.

[14] Molls, T. and Chaudhry, M.H., (1995) : Depth-averaged open-channel flow model, Journal of Hydraulic Engineering, ASCE, 121(6), pp.453-465.

[15] Rozovskii, I.L., (1961) : Flow of water in bends of open channels, Academy of Science of Ukrainian SSR, Russia.

[16] Struiksma, N., Olesen, K.W., Flokstra, C., and De Vriend, H.J., (1985) : Bed deformation in curved alluvial channels, Journal of Hydraulic Research, 23(1), pp.57-79.

[17] Sutmuller, A.M. and Glerum, H.L., (1980) : Description and evaluation of measurements carried out in a bend flume with sand bed, Report No. 14710101, Dept. of Civil Eng., Delft Univ. Tech.

[18] Wu, W., (2004) : Depth-averaged two-dimensional numerical modeling of unsteady flow and nonuniform sediment transport in open channels, Journal of Hydraulic Engineering, ASCE, 130(10), pp.1013-1024.

[19] Wu, W., Rodi, W., and Wenka, T., (2000) : 3d numerical modeling of flow and sediment transport in open channels, Journal of Hydraulic Engineering, ASCE, 126(1), pp.4-15.

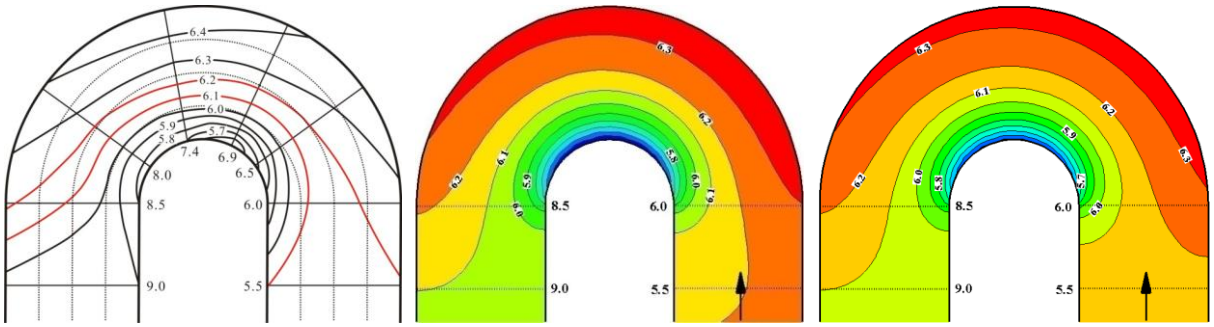

(a) Experiment (b) without dispersion stress (c) with dispersion stress

Figure 1. Measured and simulated water surface distribution (contour unit : cm) of Rozovskii's experiment

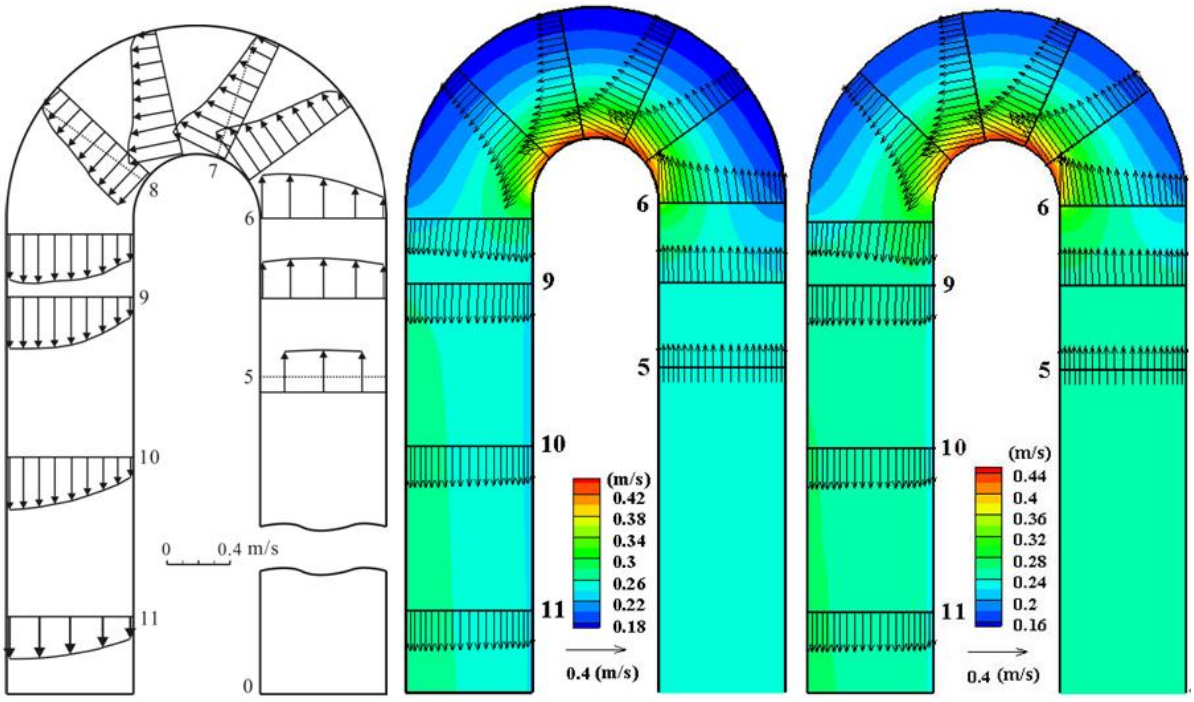

(a) Experiment (b) without dispersion stress (c) with dispersion stress

Figure 2. Measured and simulated velocity distribution of Rozovskii's experiment

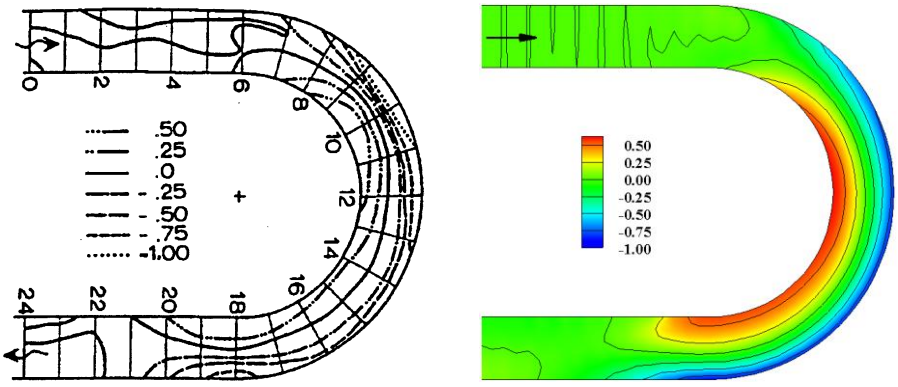

(a) Experiment (b) Simulated

Figure 3. Measured and simulated bed elevation change of LFM

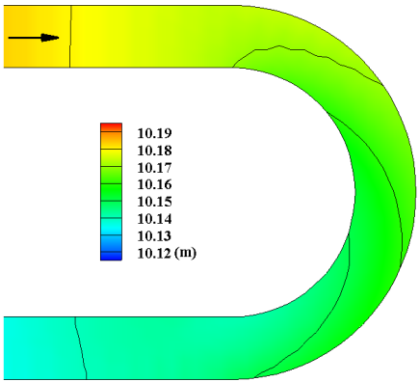

Figure 4. Simulated water surface distribution of LFM after the equilibrium state